DOI:10.1021/jf903334g

JOURNAL OF AGRICULTURAL AND FOOD CHEMISTRY
ARTICLE

# Dammarane-Type Saponins from the Flower Buds of *Panax ginseng* and Their Intracellular Radical Scavenging Capacity

Nguyen Huu Tung,[†] Gyu Yong Song,[†] Nguyen Xuan Nhiem,[†] Yan Ding,[†] Bui Huu Tai,[†] Long Guo Jin,[†] Chae-Moon Lim,[‡] Jin Won Hyun,[‡] Chun Jung Park,[§] Hee Kyoung Kang,[‡] and Young Ho Kim*,[†]

[†]College of Pharmacy, Chungnam National University, Daejeon 305-764, Korea, [‡]School of Medicine and Institute of Medical Science, Cheju National University, Jeju-si 690-756, Korea, and [§]Geumsan Ginseng Cooperative Association, Geumsan-Gun 312-800, Korea

Korean ginseng (*Panax ginseng* C.A. Meyer) has been extensively used as a functional food for thousands of years. This study with the aim to evaluate the potential of *P. ginseng* flower components as a functional food with medicinal properties resulted in the identification of three new dammarane-type saponins, named floralginsenosides Ka−Kc (**1**−**3**), along with seventeen known ones (**4**−**20**). Their structures were elucidated on the basis of chemical and spectroscopic methods, and their antioxidant activities were evaluated by the intracellular ROS radical scavenging DCF-DA assay. Among them, floralginsenoside Ka (**1**) displayed potent scavenging activity with the inhibition value of 64% at 10 $\mu$M; and ginsenoside $Rb_1$ (**13**), floralginsenoside Kc (**3**), floralginsenoside Kb (**2**), vinaginsenoside $R_9$ (**11**), majoroside $F_1$ (**12**), ginsenoside I (**17**), and ginsenoside II (**18**) showed moderate scavenging capacity with the inhibition rate of 28, 33, 35, 35, 35, 38, and 38% at 10 $\mu$M, respectively. These results warrant further studies concerning the potential of saponin extracts of *P. ginseng* flowers for functional foods.

**KEYWORDS: *Panax ginseng*; araliaceae; ginsenoside; floralginsenoside; dammarane-type triterpene; antioxidant; DCF-DA method**

## INTRODUCTION

Oxidative stress, generated by oxygen radicals, has been linked to several cellular toxicity processes, including damage to proteins, membrane lipid peroxidation, DNA alteration, and enzyme inactivation (*1*, *2*). These may be attributed to chemical carcinogenesis, heart diseases, reperfusion injury, rheumatoid arthritis, inflammation, and aging (*3*). It is well recognized that a dietary intake of antioxidant-containing foods might lower the risk of certain pathophysiologies associated with oxidative stress.

Korean ginseng (*Panax ginseng* C.A. Meyer) is an herbal root that has been broadly used as a functional food in forms of boiled extract, powder, tea, tablet, capsule, etc. for thousands of years (*4*). These conventional ginseng products are reported to have a wide range of pharmacological and physiological actions, such as antiaging, antidiabetic, anticarcinogenic, analgesic, antipyretic, antistress, antifatigue, and tranquilizing properties and promotion of DNA, RNA, and protein synthesis (*5*−*10*), which have been closely linked to ginseng's protective effects against free radical attack (*11*−*13*). Biologically active constituents of ginseng have been pursued extensively, and many dammarane-type triterpene oligoglycosides, generally known as ginsenosides, have been characterized as the principal ingredients (*14*, *15*). Recently, chemical components of the leaves and flower buds of *P. ginseng* have been reported including also various dammarane-type saponins, even several new compounds (*16*−*19*). This suggested that saponin extracts of leaves and flowers of *P. ginseng* could be a supplementary source of ginseng saponins.

There have been reports on antioxidant effects of ginsenosides. Ginsenoside $Rb_1$ was found to interact with $^{\bullet}OH$ and protect ischemic neurons (*20*), and ginsenoside Rd was reported to attenuate oxidative damage related to aging in senescene-accelerated mice (*21*). Ginsenosides $Rb_1$ and Rc showed a tendency to increase glutathione peroxidase activity, and ginsenoside Re significantly decreased Cu, Zn-superoxide dismutase activity. Also, ginsenoside $Rh_2$ remarkably increased catalase activity (*22*). Nevertheless, previous studies have demonstrated that ginsenosides had no effect on direct radicals scavenging activity (*23*−*25*). Therefore, it is insufficient to use direct radical scavenging assays for antioxidant evaluation of ginsenosides.

In this regard, the intracellular reactive oxygen species (ROS) radical scavenging DCF-DA assay, an *in vitro* cell-based method that can reproduce oxidative stress in various cell systems, could more sensitively and efficiently evaluate the efficacy of antioxidants (*26*).

The aim of this study to evaluate the potential of *P. ginseng* flower components as a functional food with medicinal properties led to the isolation of three new dammarane-type saponins, floralginsenosides Ka (**1**), Kb (**2**), and Kc (**3**), together with seventeen known ones (**4**−**20**). Their antioxidative activities were

*To whom correspondence should be addressed: College of Pharmacy, Chungnam National University, Daejeon 305-764, Korea. Tel: +82-42-821-5933. Fax: +82-42-823-6566. E-mail: yhk@cnu.ac.kr.

 Published on Web 12/23/2009 

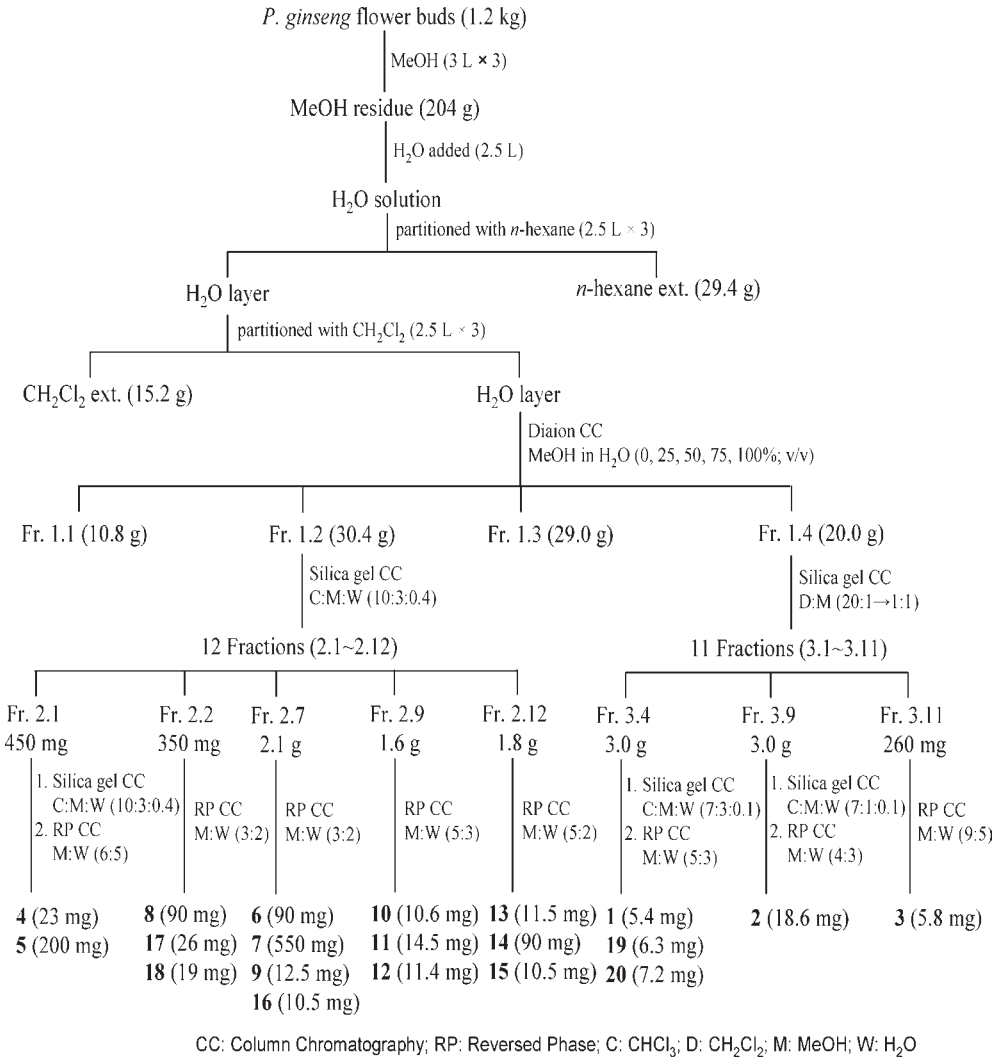


**Figure 1.** Purification of ginsenosides **1**−**20**.

particularly determined using the intracellular ROS radical scavenging DCF-DA assay.

## MATERIALS AND METHODS

**General Procedures.** Optical rotations were obtained on a DIP-360 digital polarimeter (Jasco, Easton, MD). IR spectra were measured on a Perkin-Elmer 577 spectrometer (Perkin-Elmer, Waltham, MA) using KBr pellets. Nuclear magnetic resonance (NMR) spectra were recorded on Bruker DRX 400 and 500 NMR spectrometers (Bruker, Billerica, MA), respectively, using Bruker's standard pulse program, with tetramethylsilane as the internal standard and chemical shift values were expressed in $\delta$ (ppm). Electrospray ionization (ESI) mass spectrometry (MS) spectra were recorded on a model 1100 LC-MSD trap spectrometer (Agilent, Santa Clara, CA). High-resolution electrospray ionization time-of-flight MS (HRESITOFMS) measurements utilized a JEOL AccuTOF LC mass spectrometer (Jeol, Tokyo, Japan), equipped with an electrospray ion source. Gas chromatography (GC) (Shimadzu-2010, Tokyo, Japan), equipped with a DB-05 capillary column (30 m × 0.5 mm i.d.) and a flame ionization detector (FID) [column temperature, 210 °C; FID detector temperature, 300 °C; injector temperature, 270 °C; He carrier-gas flow rate, 30 mL/min (splitting ratio: 1/20)], was used for sugar determination. Column chromatography (CC) was performed on silica gel (70−230 and 230−400 mesh, Merck), YMC RP-18 resins (30−50 $\mu$m, Fuji Silysia Chemical Ltd., Aichi, Japan), and Diaion HP-20 (Mitshubishi Chemical, Tokyo, Japan). TLC was performed on Kieselgel 60 $F_{254}$ (1.05715; Merck, Darmstadt, Germany) or RP-18 $F_{254s}$ (Merck) plates. Spots were visualized by spraying with 10% aqueous $H_2SO_4$ solution, followed by heating.

**Plant Material.** The flower buds of *P. ginseng* were collected in Gaeumsan province, Korea, in August 2008, and taxonomically identified by one of us (Y.H.K.). The voucher specimens have been deposited at the College of Pharmacy, Chungnam National University, Korea.

**Extraction and Isolation.** The air-dried flower buds of *P. ginseng* (1.2 kg) were extracted in MeOH (3 L × 3, 50 °C), and the combined extracts were concentrated *in vacuo*. The MeOH residue (204 g) was suspended in $H_2O$ (2.5 L) and then partitioned with *n*-hexane and $CH_2Cl_2$ (each 2.5 L × 3), successively, to obtain *n*-hexane and $CH_2Cl_2$-soluble fractions in the weights of 29.4 g, 15.2 g, and the water layer, which was subjected to a Diaion HP-20 column eluted stepwise by the mixture of MeOH and $H_2O$ (25, 50, 75, and 100% MeOH; v/v) to give four fractions (fr. 1.1−fr. 1.4). The detailed separation process is shown as **Figure 1**.

**Floralginsenoside Ka (1):** white amorphous powder; $[\alpha]_D^{20}$ +6° (*c* 0.05, MeOH); IR (KBr) $\nu_{max}$ 3456, 2915, 1648, 1252, and 1062 $cm^{-1}$; $^1H$ and $^{13}C$ NMR data, see **Tables 1**−**3**; ESI-MS (negative ion mode) *m*/*z* 653 $[M - OH]^-$, 651 $[M - H_2O - H]^-$, 637 $[M - OOH]^-$, 489 $[M - H_2O - C_6H_{10}O_5 - H]^-$; HRESITOFMS (negative ion mode) *m*/*z* 651.4116 $[(M - H_2O) - H]^-$ (calcd for $C_{36}H_{59}O_{10}$, 651.4108).

**Floralginsenoside Kb (2):** white amorphous powder; $[\alpha]_D^{20}$ +12° (*c* 0.08, MeOH); IR (KBr) $\nu_{max}$ 3446, 2913, 1738, 1262, and 1064 $cm^{-1}$; $^1H$ and $^{13}C$ NMR data, see **Tables 1**−**3**; ESI-MS (negative ion mode) *m*/*z* 919 $[M - H]^-$, 757 $[M - C_6H_{10}O_5 - H]^-$, 433 $[M - 3C_6H_{10}O_5 - H]^-$; HRESI-TOFMS (negative ion mode) *m*/*z* 919.4899 $[M - H]^-$ (calcd for $C_{45}H_{75}O_{19}$, 919.4903).

**Floralginsenoside Kc (3):** white amorphous powder; $[\alpha]_D^{20}$ +11° (*c* 0.10, MeOH); IR (KBr) $\nu_{max}$ 3452, 2918, 1743, 1262, and 1058 $cm^{-1}$; $^1H$ and $^{13}C$ NMR data, see **Tables 1**−**3**; ESI-MS (negative ion mode) *m*/*z* 917

**Table 1.** $^{13}C$ NMR Data for Compounds **1**−**3** in Pyridine-$d_5$

| position | **1**[a] | **2**[b] | **3**[a] |
|---|---|---|---|
| 1 | 39.8 | 39.4 | 39.6 |
| 2 | 28.6 | 26.9 | 27.1 |
| 3 | 78.9 | 89.2 | 89.4 |
| 4 | 40.8 | 39.9 | 40.1 |
| 5 | 62.2 | 56.6 | 56.8 |
| 6 | 68.2 | 18.7 | 18.9 |
| 7 | 47.9 | 35.4 | 35.5 |
| 8 | 41.7 | 40.3 | 40.5 |
| 9 | 50.4 | 50.5 | 50.6 |
| 10 | 39.8 | 37.1 | 37.3 |
| 11 | 31.2 | 31.0 | 31.2 |
| 12 | 70.7 | 70.3 | 70.5 |
| 13 | 49.6 | 49.9 | 50.1 |
| 14 | 51.8 | 51.7 | 50.6 |
| 15 | 31.5 | 31.0 | 31.2 |
| 16 | 27.1 | 26.9 | 27.2 |
| 17 | 52.0 | 52.0 | 51.9 |
| 18 | 18.1 | 16.2 | 16.4 |
| 19 | 18.0 | 16.5 | 16.7 |
| 20 | 83.7 | 82.8 | 84.0 |
| 21 | 23.0 | 22.3 | 23.0 |
| 22 | 33.3 | 28.3 | 40.1 |
| 23 | 27.1 | 39.7 | 60.7 |
| 24 | 90.5 | 203.4 | 203.5 |
| 25 | 146.6 | | |
| 26 | 113.8 | | |
| 27 | 18.2 | | |
| 28 | 32.5 | 28.3 | 28.5 |
| 29 | 17.0 | 16.9 | 17.0 |
| 30 | 17.9 | 17.7 | 17.8 |
| Glc-1′ | 98.7 | 105.4 | 105.5 |
| Glc-2′ | 75.6 | 83.8 | 83.0 |
| Glc-3′ | 78.7 | 78.4 | 78.4 |
| Glc-4′ | 72.2 | 71.9 | 72.1 |
| Glc-5′ | 79.7 | 78.2 | 78.8 |
| Glc-6′ | 63.4 | 63.1 | 63.3 |
| Glc-1″ | | 106.4 | 106.5 |
| Glc-2″ | | 77.4 | 77.6 |
| Glc-3″ | | 79.6 | 79.8 |
| Glc-4″ | | 71.9 | 72.1 |
| Glc-5″ | | 78.5 | 78.5 |
| Glc-6″ | | 62.9 | 63.2 |
| Glc-1‴ | | 98.4 | 98.5 |
| Glc-2‴ | | 75.3 | 75.4 |
| Glc-3‴ | | 78.2 | 78.4 |
| Glc-4‴ | | 71.9 | 72.1 |
| Glc-5‴ | | 78.6 | 78.6 |
| Glc-6‴ | | 63.1 | 63.2 |

[a] Recorded at 125 MHz. [b] Recorded at 100 MHz.

**Table 2.** $^1H$ NMR Data for the Aglycon Moieties of Compounds **1**−**3** in Pyridine-$d_5$

| position | **1**[a] | **2**[b] | **3**[a] |
|---|---|---|---|
| 1 | 1.03 m | 0.74 m | 0.75 m |
| | 1.74 m | 1.50 m | 1.51 m |
| 2 | 1.88 m | 1.82 m | 1.83 m |
| | 1.97 m | 2.20 m | 2.21 m |
| 3 | 3.54 dd (4.5, 11.5) | 3.26 dd (4.4, 11.6) | 3.28 dd (4.5, 11.5) |
| 4 | | | |
| 5 | 1.22 d (10.0) | 0.66 m | 0.67 m |
| 6 | 4.42 m | 1.36 m | 1.36 m |
| | | 1.50 m | 1.50 m |
| 7 | 1.88 m | 1.22 m | 1.21 m |
| | 1.98 m | 1.45 m | 1.45 m |
| 8 | | | |
| 9 | 1.58 m | 1.36 m | 1.36 m |
| 10 | | | |
| 11 | 1.36 m | 1.41 m | 1.42 m |
| | 2.12 m | 1.92 m | 1.92 m |
| 12 | 4.12 m | 4.14 m | 4.15 m |
| 13 | 2.03 m | 1.98 m | 2.00 m |
| 14 | | | |
| 15 | 1.09 m | 1.02 m | 1.02 m |
| | 1.60 m | 1.55 m | 1.56 m |
| 16 | 1.36 m | 1.84 m | 1.83 m |
| | 1.82 m | 2.20 m | 2.20 m |
| 17 | 2.58 m | 2.62 m | 2.61 m |
| 18 | 1.11 s | 0.97 s | 0.96 s |
| 19 | 1.03 s | 0.84 s | 0.84 s |
| 20 | | | |
| 21 | 1.63 s | 1.53 s | 1.53 s |
| 22 | 2.20 m | 1.95 m | 2.73 m |
| | 2.48 m | 2.74 m | 2.96 m |
| 23 | 1.82 m | 2.65 m | 4.07 dd (7.0, 14.0) |
| | 2.21 m | 2.95 m | |
| 24 | 4.73 m | 9.81 br s | 9.81 br s |
| 25 | | | |
| 26 | 5.04 br s | | |
| | 5.21 br s | | |
| 27 | 1.90 s | | |
| 28 | 2.01 s | 1.29 s | 1.30 s |
| 29 | 1.47 s | 1.13 s | 1.13 s |
| 30 | 0.97 s | 0.96 s | 0.95 s |

[a] Recorded at 500 MHz. [b] Recorded at 400 MHz.

$[M - H_2O - H]^-$, 755 $[M - H_2O - C_6H_{10}O_5 - H]^-$; HRESITOFMS (negative ion mode) $m/z$ 917.4734 $[(M - H_2O) - H]^-$ (calcd for $C_{45}H_{73}O_{19}$, 917.4746).

**Acid Hydrolysis of Compounds 1−3 and Sugar Determination.** A solution of each (3.0 mg) in 1.0 M HCl (3.0 mL) was heated under reflux for 2 h. Then, the reaction mixture was concentrated *in vacuo* to dryness. The residue was extracted with EtOAc and $H_2O$ (5 mL × 3). Next, the sugar residue, obtained by concentration of the water layer, was dissolved in dry pyridine (0.1 mL). Then, L-cysteine methyl ester hydrochloride in pyridine (0.06 M, 0.1 mL) was added to the solution. After heating the reaction mixture at 60 °C for 2 h, 0.1 mL of trimethylsilylimidazole was added. Heating at 60 °C was continued for a further 2 h, and the mixture was evaporated to give a dried product, which was partitioned between hexane and $H_2O$. After that, the hexane layer was analyzed by the GC procedure (General Procedures). The peak of the hydrolysate of the sample was detected at $t_R$ 14.12 min for D-glucose. The retention times for the authentic samples (Sigma), after being treated in the similar manner, were 14.12 min (D-glucose) and 14.25 min (L-glucose). Co-injection of the hydrolysates of the sample with standard D-glucose gave single peaks.

**Antioxidant Assay.** *Chemicals and Sample Preparation*. 2′,7′-dichlorofluorescin diacetate (DCF-DA), *N*-acetylcysteine (NAC), and glucose were purchased from Sigma (St. Louis, MO). All other chemicals and reagents were of analytical grade. The tested compounds (**1**−**20**), glucose, and NAC were dissolved in DMSO.

*Cell Culture*. V79-4 Chinese hamster lung fibroblast cells were obtained from the American Type Culture Collection (Rockville, MD). The cells were maintained in Dulbecco's modified Eagle's medium supplemented with streptomycin (100 μg/mL), penicillin (100 units/mL), and 10% heat-inactivated fetal calf serum at 37 °C in humidified atmosphere of 5% $CO_2$.

*Intracellular ROS Measurement*. The DCF-DA method was used to detect intracellular ROS. Briefly, DCF-DA diffuses into cells, where it is further hydrolyzed by intracellular esterase to polar 2′,7′-dichlorodihydrofluorescein. This nonfluorescent fluorescein analogue is trapped in cells and can be oxidized to the highly fluorescent 2′,7′-dichlorofluorescein by intracellular oxidants (*26*). Thus, the dichlorofluorescein is directly proportional to the amount of intracellular radical generation. V79-4 cells were seeded at a density of $1 \times 10^5$ cells/mL in 96 well plates. Sixteen hours later, the V79-4 cells were treated with samples at the final concentration of 10 μM, followed by the addition of 1 mM $H_2O_2$ 30 min later. The final DMSO concentration was kept at 0.1% in order to not affect cell viability.

**Table 3.** $^1$H NMR Data for the Sugar Moieties of Compounds **1**−**3** in Pyridine-$d_5$

| position | **1**[a] | **2**[b] | **3**[a] |
|---|---|---|---|
| Glc-1′ | 5.20 d (8.0) | 4.94 d (7.6) | 4.94 d (7.5) |
| Glc-2′ | 4.01 t (8.5) | 4.23 m | 4.24 m |
| Glc-3′ | 4.27 m | 4.24 m | 4.25 m |
| Glc-4′ | 4.20 m | 4.13 m | 4.15 m |
| Glc-5′ | 3.96 m | 3.93 m | 3.94 m |
| Glc-6′ | 4.30 m | 4.34 m | 4.34 m |
| | 4.50 br d(11.5) | 4.57 br d (12.0) | 4.58 br d (11.0) |
| Glc-1″ | | 5.38 d (7.2) | 5.39 d (8.0) |
| Glc-2″ | | 4.11 m | 4.12 m |
| Glc-3″ | | 4.29 m | 4.30 m |
| Glc-4″ | | 4.33 m | 4.33 m |
| Glc-5″ | | 3.94 m | 3.94 m |
| Glc-6″ | | 4.36 m | 4.36 m |
| | | 4.49 m | 4.50 m |
| Glc-1‴ | | 5.15 d (8.0) | 5.16 d (8.0) |
| Glc-2‴ | | 4.01 m | 4.02 m |
| Glc-3‴ | | 4.26 m | 4.27 m |
| Glc-4‴ | | 4.20 m | 4.22 m |
| Glc-5‴ | | 3.97 m | 3.97 m |
| Glc-6‴ | | 4.33 m | 4.33 m |
| | | 4.50 m | 4.50 m |

[a] Recorded at 500 MHz. [b] Recorded at 400 MHz.

Next, cells were further incubated for 30 min at 37 °C. Finally, the fluorescence of 2′,7′-dichlorofluorescein was detected at an excitation wavelength of 485 nm and an emission wavelength of 535 nm using a Perkin-Elmer LS-5B spectrofluorometer. The ROS scavenging activity was expressed as the inhibition rate (%), which was calculated from the following formula:

$$\text{ROS scavenging activity } (\%) = [(\text{OD}_{\text{control}} - \text{OD}_{\text{sample}})/\text{OD}_{\text{control}}] \times 100$$

*Statistical Analysis*. The data were presented as mean ± standard error (SE) of three different experiments in triplicate. The results were subjected to an analysis of the variance (ANOVA) using the Tukey test to analyze the difference. $p < 0.05$ were considered significantly.

## RESULTS AND DISCUSSION

**Isolation and Structure Elucidation of Compounds.** The methanolic extract of the flower buds of *P. ginseng* was suspended in $H_2O$ and partitioned successively with *n*-hexane and $CH_2Cl_2$. The $H_2O$ layer was subjected to a Diaion HP-20 column, followed by various silica gel and YMC reversed-phase columns to yield three new dammarane-type saponins, floralginsenosides Ka−Kc (**1**−**3**) (**Figure 2**), and seventeen known ones (**4**−**20**) (Figure S1 in the Supporting Information).

The known saponins were identified as ginsenoside $M_{7cd}$ (**4**) (*16*), ginsenoside $Rg_1$ (**5**) (*27*), floralginsenoside J (**6**) (*17*), ginsenoside Re (**7**) (*27*), ginsenoside $F_5$ (**8**) (*18*), vinaginsenoside $R_{15}$ (**9**) (*18*), vinaginsenoside $R_4$ (**10**) (*28*), vinaginsenoside $R_9$ (**11**) (*28*), majoroside $F_1$ (**12**) (*28*), ginsenoside $Rb_1$ (**13**) (*18*), floralginsenoside La (**14**) (*17*), floralginsenoside Lb (**15**) (*17*), floralginsenoside B (**16**) (*18*), ginsenoside I (**17**) (*29*), ginsenoside II (**18**) (*29*), floralginsenoside M (**19**) (*19*), and floralginsenoside N (**20**) (*19*), respectively, on the basis of NMR, ESI-MS data, and comparison with those reported in the literature. To the best of our knowledge, ginsenoside $M_{7cd}$ (**4**), vinaginsenoside $R_{15}$ (**9**), vinaginsenoside $R_9$ (**11**), and majoroside $F_1$ (**12**) were isolated for the first time from flower buds of *P. ginseng*.

Floralginsenoside Ka (**1**), an amorphous powder, has the molecular formula $C_{36}H_{62}O_{11}$ deduced by a HRESITOFMS experiment (found at *m*/*z* [(M − $H_2O$) − H]$^-$ 651.4116, calcd for $C_{36}H_{59}O_{10}$ 651.4108). It was proposed to have a hydroperoxy group due to the positive response to *N*,*N*-dimethyl-*p*-phenylenediammonium dichloride reagent (*30*). In addition, the negative ESI-MS of **1** revealed the fragment ion peaks at *m*/*z* 653 [M − OH]$^-$, *m*/*z* 651 [M − $H_2O$ − H]$^-$, *m*/*z* 637 [M − OOH]$^-$, and *m*/*z* 489 [M − $H_2O$ − $C_6H_{10}O_5$ − H]$^-$, respectively. The IR spectrum of **1** showed absorption bands at $\nu_{max}$ 3456, 1648, and 1062 cm$^{-1}$ due to hydroxy groups, double bond, and glycosidic linkage. Acid hydrolysis of **1** liberated D-glucose confirmed by GC analysis. From the $^1$H and $^{13}$C NMR spectra (**Tables 1**−**3**), compound **1** was proposed to be a β-D-glucopyranosyl unit and an aglycon with five oxygenated carbons and one double bond. The configuration of the anomeric position was determined to be β on the basis of the large coupling constant ($J$ = 8.0 Hz) of the anomeric proton at $\delta_H$ 5.20 in the $^1$H NMR spectrum of **1**. In addition, the $^1$H NMR spectrum of **1** showed signals assignable to the aglycon part [$\delta_H$ 0.97, 1.03, 1.11, 1.47, 1.63, 1.90, 2.01 (3H each, all s, $H_3$-30,19,18,29,21,27,28); 3.54 (1H, dd, $J$ = 4.5, 11.5 Hz, H-3), 4.12 (1H, m, H-12), 4.42 (1H, m, H-6), 4.73 (1H, m, H-24), 5.04 and 5.21 (1H each, all br s, H-26)]. The $^{13}$C NMR spectrum of **1** disclosed thirty-six carbon signals including the set of six signals ($\delta_C$ 98.7, 75.6, 78.7, 72.2, 79.7, and 63.4) revealing to a β-D-glucopyranosyl unit, and thirty remaining ones of a sapogenol moiety were similar to those of floralginsenoside C (*18*). Furthermore, the structure of **1** was assigned by the $^1$H−$^1$H COSY, HMQC, and HMBC spectra, respectively. As shown in **Figure 3**, the $^1$H−$^1$H COSY experiment on **1** indicated the presence of partial structures written in bold lines, and in the HMBC spectrum, the long-range correlations were observed between the following protons and carbons: H-6 and C-8; H-12 and C-9,13,17; H-17 and C-20; H-18 and C-7,9,14; H-19 and C-1,5,9,10; H-21 and C-17,22; H-22 and C-24; H-24 and C-27; H-26 and C-24,27; H-27 and C-24,26; H-1′ and C-20. Consequently, the structure of floralginsenoside Ka (**1**) was characterized as 3β,6α,12β,20β-tetrahydroxy-24ξ -hydroperoxy-dammar-25(26)-ene 20-*O*-β-D-glucopyranoside.

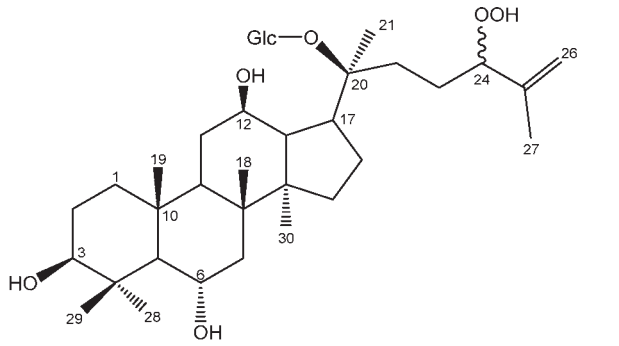


Floralginsenoside Ka (**1**)

| | R |
|---|---|
| Floralginsenoside Kb (**2**) | H |
| Floralginsenoside Kc (**3**) | OH |

**Figure 2.** The structures of new floralginsenosides **1**−**3**.

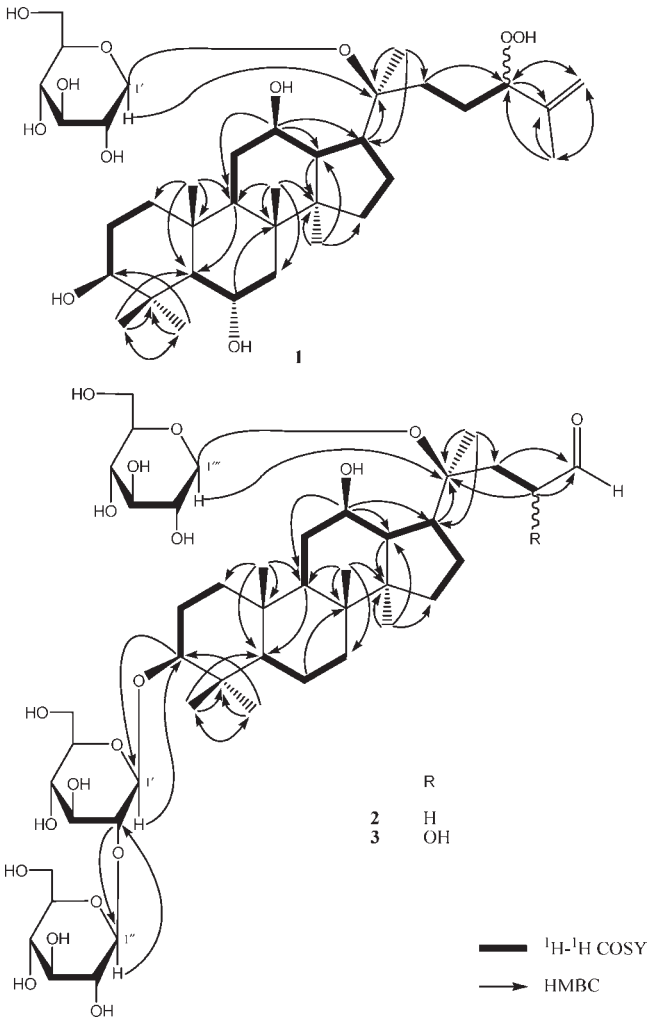


**Figure 3.** Significant $^1$H−$^1$H COSY and HMBC correlations for new floralginsenosides **1**−**3**.

Floralginsenoside Kb (**2**), also an amorphous powder, has the molecular formula $C_{45}H_{76}O_{19}$ based on a HRESITOFMS experiment (found at $m/z$ [M − H]$^-$ 919.4899, calcd for $C_{45}H_{75}O_{19}$ 919.4903). In the negative ESI-MS of **2**, a quasimolecular ion peak at $m/z$ 919 [M − H]$^-$ and the fragment ion peaks at $m/z$ 757 [M − $C_6H_{10}O_5$ − H]$^-$ and $m/z$ 433 [M − 3$C_6H_{10}O_5$ − H]$^-$ were observed. The IR spectrum of **2** exhibited absorption bands at $\nu_{max}$ 3446, 1738, and 1064 cm$^{-1}$ due to hydroxy groups, carbonyl function, and glycosidic linkage. The acid hydrolysis of **2** liberated D-glucose identified by GC analysis. The $^1$H NMR (pyridine-$d_5$) spectrum of **2** (**Tables 2** and **3**) showed six methyl singlets [$\delta_H$ 0.84, 0.96, 0.97, 1.13, 1.29, 1.53 (3H each, all s, $H_3$-19,30,18,29,28,21), two oxymethine protons [$\delta_H$ 3.26 (dd, $J$ = 4.4, 11.6 Hz, H-3), 4.14 (m, H-12)], three anomeric signals [$\delta_H$ 4.94 (d, $J$ = 7.6 Hz, H-1′), 5.15 (d, $J$ = 8.0 Hz, H-1‴), 5.38 (d, $J$ = 7.2 Hz, H-1″], and an aldehyde proton ($\delta_H$ 9.81, br s, H-24). The $^{13}$C NMR spectrum of **2** (**Table 1**) disclosed 45 signals including three oxygenated carbons [$\delta_C$ 70.3, 82.8, 89.2 (C-12,20,3)], three anomeric signals [$\delta_C$ 98.4, 105.4, 106.4 (C-1‴,1′,1″), and an aldehyde carbonyl carbon ($\delta_C$ 203.4, C-24). In addition, the signal of C-5 at $\delta_C$ 56.6 in the $^{13}$C NMR spectrum of **2** is a characteristic of a protopanaxadiol-type aglycon common among dammarane-type saponins in *P. ginseng* with variations in its side chain. Furthermore, the $^1$H and $^{13}$C NMR data of **2** were similar to those of ginsenoside Rd (*31*), except for the signals belonging to the side-chain moiety (C-22 part) of the aglycon, which was composed of, notably, only two methylene and one aldehyhyde carbons. The structure of **2**, especially the side chain, was assigned by the $^1$H−$^1$H COSY, HMQC, and HMBC spectra, respectively. As shown in **Figure 3**, the $^1$H−$^1$H COSY experiment on **2** indicated the presence of partial structures written in bold lines, and in the HMBC spectrum, the long-range correlations were observed between the following protons and carbons: H-3 and C-1′, H-12 and C-9,13,17; H-18 and C-7,9,14; H-19 and C-1,5,9,10; H-21 and C-17,20,22; H-22 and C-24; H-23 and C-20,24; H-30 and C-13,15; H-1′ and C-3; H-2′ and C-1″; H-1″ and C-2′; H-1‴ and C-20. Thus, the structure of floralginsenoside Kb (**2**) was established as 3-*O*-[*β*-D-glucopyranosyl-(1→2)-*β*-D-glucopyranosyl]-20-*O*-*β*-D-glucopyranosyl-3*β*,12*β*,20*β*-trihydroxy-25,26,27-trinordammar-24-al.

Floralginsenoside Kc (**3**), an amorphous powder, has the molecular formula $C_{45}H_{76}O_{20}$ by a HRESITOFMS experiment (found at $m/z$ [(M − $H_2O$) − H]$^-$ 917.4734, calcd for $C_{45}H_{73}O_{19}$ 917.4746). Additionally, the negative ESI-MS of **3** exhibited the fragment ion peaks at $m/z$ 917 [M − $H_2O$ − H]$^-$ and $m/z$ 755 [M − $H_2O$ − $C_6H_{10}O_5$ − H]$^-$, respectively. The IR spectrum of **3** displayed absorption bands at $\nu_{max}$ 3452, 1743, and 1058 due to hydroxy groups, carbonyl function, and glycosidic linkage. The acid hydrolysis of **3** liberated D-glucose. The $^1$H and $^{13}$C NMR data (**Tables 1**−**3**) of **3** resembled to those of floralginsenoside Kb (**2**) as above, except for the signals of the side-chain moiety (C-23,24,25) with the appearance of one oxygenated methine carbon [$\delta_C$ 60.7 and $\delta_H$ 4.07 (1H, dd, $J$ = 7.0, 14.0 Hz)] in **3** instead of the methylene carbon C-23 in **2**. Furthermore, the structure of **3**, especially the side chain, was assigned by means of the $^1$H−$^1$H COSY, HMQC, and HMBC spectra, respectively. As shown in **Figure 3**, the $^1$H−$^1$H COSY spectrum of **3** indicated the presence of partial structures written in bold lines, and in the HMBC experiment, the long-range correlations were observed between the following protons and carbons: H-3 and C-1′, H-12 and C-9,13,17; H-18 and C-7,8,9,14; H-19 and C-1,5,9,10; H-21 and C-17,20,22; H-22 and C-24; H-23 and C-20,24; H-30 and C-13,15; H-1′ and C-3; H-2′ and C-1″; H-1″ and C-2′; H-1‴ and C-20. Hence, floralginsenoside Kc (**3**) was identified as 3-*O*-[*β*-D-glucopyranosyl-(1→2)-*β*-D-glucopyranosyl]-20-*O*-*β*-D-glucopyranosyl-3*β*,12*β*,20*β*,23*ξ*-tetrahydroxy-25,26,27-trinordammar-24-al.

**Antioxidant Evaluation of Compounds.** The antioxidant activity of the ginsenosides (**1**−**20**) was evaluated by the intracellular ROS radical scavenging DCF-DA method. Oxidative stress was induced in V79-4 Chinese hamster lung fibroblast cells by exposure to $H_2O_2$, one of common ROS in physiological systems. The reduction of oxidative stress was based on the intracellular ROS scavenging capacity as described in Materials and Methods. In order to confirm the antioxidant activity of tested compounds, cell viability was simultaneously determined using the colorimetric MTT [3-(4,5-dimethylthiazole-2-yl)-2,5-diphenyltetrazolium bromide] assay (*32*), and as a result, no cytotoxicity was found (data not shown). Glucose was used as negative control, which showed the intracellular ROS scavenging capacity of 2.6%. Of the isolates, notably, floralginsenoside Ka (**1**) (10 $\mu$M) displayed potent scavenging activity with the inhibition value of 64%, whereas ginsenoside $Rb_1$ (**13**), floralginsenoside Kc (**3**), floralginsenoside Kb (**2**), vinaginsenoside $R_9$ (**11**), majoroside $F_1$ (**12**), ginsenoside I (**17**), and ginsenoside II (**18**) showed moderate scavenging capacity with inhibition rates of 28, 33, 35, 35, 35, 38, and 38%, respectively. Besides, the others exhibited negligible scavenging activities with inhibition values less than 10% as compared with NAC, which was used as positive control (91%) at the same concentration (**Figure 4**).

Structurally, ginsenosides **1**−**20** are classified into either 20*S*-protopanaxadiol (PPD) type, including floralginsenoside

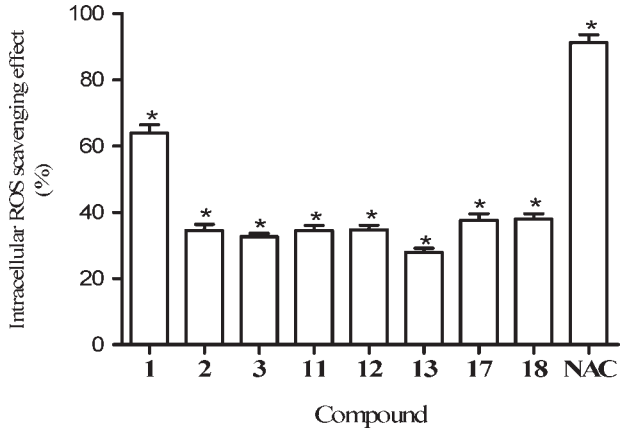


**Figure 4.** The scavenging effect of **1**−**3**, **11**−**13**, **17**, and **18** at 10 $\mu$M on intracellular ROS. The cells were treated with the samples at 10 $\mu$M. After 30 min, $H_2O_2$ (1 mM) was added to the plate. After 30 min, DCF-DA was added and the intracellular ROS generated were detected by spectrofluorometry. *Significantly different from control cells ($p < 0.05$) as examined by Tukey test. NAC was used as positive control.

Ka (**1**), floralginsenoside Kb (**2**), floralginsenoside Kc (**3**), vinaginsenoside $R_9$ (**11**), majoroside $F_1$ (**12**), ginsenoside $Rb_1$ (**13**), ginsenoside I (**17**), and ginsenoside II (**18**) or 20*S*-protopanaxatriol (PPT) type, including ginsenoside $M_{7cd}$ (**4**), ginsenoside $Rg_1$ (**5**), floralginsenoside J (**6**), ginsenoside Re (**7**), ginsenoside $F_5$ (**8**), vinaginsenoside $R_{15}$ (**9**), vinaginsenoside $R_4$ (**10**), floralginsenoside La (**14**), floralginsenoside Lb (**15**), floralginsenoside B (**16**), floralginsenoside M (**19**), and floralginsenoside N (**20**) with particular sugar moieties (*15*). The obtained antioxidant data suggested that the PPD-type ginsenosides were much more active than that of PPT-type ginsenosides. Moreover, this finding was consistent with the literature that there have been antioxidant ginsenosides $Rb_1$, Rd, Rc, and $Rh_2$, which are all PPD-type ginsenosides (*20*−*22*).

Particularly, floralginsenoside Ka (**1**), a PPT-type ginsenoside, showed potent intracellular ROS scavenging activity suggesting that the appearance of a hydroperoxyl group at C-24, which is reactive and might neutralize ROS, is important for its antioxidant activity. This was further supported from the observation that ginsenosides I and II possessing a similar 24-hydroperoxyl group also exhibited particular intracellular ROS scavenging capacity.

Taken together, it was indicated that the absence of 6-hydroxy group and the presence of 24-hydroperoxyl within ginsenoside structures might be responsible for the intracellular ROS scavenging activity of ginsenosides.

In conclusion, this study indicated that dammarane-type saponins are the main components of the flower buds as well as the roots of *P. ginseng*. Additionally, three new floralginsenosides Ka (**1**), Kb (**2**), and Kc (**3**), which showed significant intracellular ROS scavenging activities, were investigated, respectively. These results warrant further studies concerning potential of saponin extracts of *P. ginseng* flowers for functional foods.

## ACKNOWLEDGMENT

The authors would like to thank the Korean Basic Science Institute (KBSI) for taking NMR and MS experiments.

**Supporting Information Available:** The key spectra ($^1$H NMR, $^{13}$C NMR, and HRMS) of floralginsenosides Ka−Kc (**1**−**3**) and the structures of known ginsenosides (**4**−**20**). This material is available free of charge via the Internet at http://pubs.acs.org.

## LITERATURE CITED

(1) Cohen, G. M.; d'Arcy Doherty, M. Free radical mediated cell toxicity by redox cycling chemicals. *Br. J. Cancer* **1987**, *55*, 46–52.
(2) Di Giulio, R. T.; Washburn, P. C.; Wenning, R. J.; Winston, G. W.; Jewell, C. S. Biochemical responses in aquatic animals: A review of determinants of oxidative stress. *Environ. Toxicol. Chem.* **1989**, *8*, 1103–1123.
(3) Halliwell, B.; Gutteridge, J. M. C. Free radicals, aging and disease. In Halliwell, B., Gutteridge, J. M. C., Eds.; *Free radical in biology and medicine*; Clarendon Press: Oxford, 1989; pp 416−508.
(4) Yun, T. K. Brief introduction of *Panax ginseng* C.A. Meyer. *J. Korean Med. Sci.* **2001**, *16*, S3–S5.
(5) Abe, H.; Arichi, S.; Hayashi, T.; Odashima, S. Ultrastructural studies of Morris hepatoma cells reversely transformed by ginsenosides. *Experientia* **1979**, *35*, 1647–1649.
(6) Sugaya, A.; Yuzurihara, M.; Tsuda, T.; Yasuda, K.; Kajiwara, K.; Sugaya, E. Proliferative effect of ginseng saponin on neurite extension of primary cultured neurons of the rat cerebral cortex. *J. Ethnopharmacol.* **1988**, *22*, 173–181.
(7) Yokozawa, T.; Oura, H.; Kawashima, Y. The effect of ginsenoside-Rb2 on nitrogen balance. *J. Nat. Prod.* **1989**, *52*, 1350–1352.
(8) Bhattacharya, S. K.; Mitra, S. K. Anxiolytic activity of *Panax ginseng* root: An experimental study. *J. Ethnopharmacol.* **1991**, *34*, 87–92.
(9) Deng, H. W.; Guan, Y. Y.; Kwan, C. Y. The effects of ginsenosides on lipid peroxidation in liver and cardiac muscle homogenates. *Biochem. Arch.* **1990**, *6*, 359–365.
(10) Yokozawa, T.; Fujitsuka, N.; Yasui, T.; Oura, H. Effects of ginsenoside Rb2 on adenine nucleotide content of rat hepatic tissue. *J. Pharm. Pharmacol.* **1991**, *43*, 290–291.
(11) Chen, X. Cardiovascular protection by ginsenosides and their nitric oxide releasing action. *Clin. Exp. Pharmacol. Physiol.* **1996**, *23*, 728–732.
(12) Lee, H. J.; Kim, D. Y.; Chang, C. C. Antioxidant effects of Korean red ginseng components on the antioxidant enzymes activity and lipid peroxidation in the liver of mouse treated with paraquat. *J. Ginseng Res.* **1999**, *23*, 182–189.
(13) Maffei Facino, R.; Carini, M.; Aldini, G.; Berti, F.; Rossoni, G. *Panax ginseng* administration in the rat prevents myocardial ischemia-reperfusion damage induced by hyperbaric oxygen: Evidence for an antioxidant intervention. *Planta Med.* **1999**, *65*, 614–619.
(14) Park, J. D.; Rhee, D. K.; Lee, Y. H. Biological activities and chemistry of saponins from *Panax ginseng* C. A. Meyer. *Phytochemistry Rev.* **2005**, *4*, 159–175.
(15) Shibata, S. Chemistry and cancer preventing activities of ginseng saponins and some related triterpenoid compounds. *J. Korean Med. Sci.* **2001**, *16*, 28–37.
(16) Dou, D. Q.; Chen, Y. J.; Liang, L. H.; Pang, F. G.; Shimizu, N.; Takeda, T. Six new dammarane-type triterpene saponins from the leaves of *Panax ginseng*. *Chem. Pharm. Bull.* **2001**, *49*, 442–446.
(17) Nakamura, S.; Sugimoto, S.; Matsuda, H.; Yoshikawa, M. Structures of dammarane-type triterpene triglycosides from the flower buds of *Panax ginseng*. *Heterocycles* **2007**, *71*, 577–588.
(18) Yoshikawa, M.; Sugimoto, S.; Nakamura, S.; Matsuda, H. Medicinal flowers. XI. Structures of new dammarane-type triterpene diglycosides with hydroperoxide group from flower buds of *Panax ginseng*. *Chem. Pharm. Bull.* **2007**, *55*, 571–576.
(19) Yoshikawa, M.; Sugimoto, S.; Nakamura, S.; Sakumae, H.; Matsuda, H. Medicinal flowers. XVI. New dammarane-type triterpene tetraglycosides and gastroprotective principles from flower buds of *Panax ginseng*. *Chem. Pharm. Bull.* **2007**, *55*, 1034–1038.
(20) Lim, J. H.; Wen, T. C.; Matsuda, S.; Tanaka, J.; Maeda, N.; Peng, H.; Aburaya, J.; Ishihara, K.; Sakanaka, M. Protection of ischemic hippocampal neurons by ginsenoside $Rb_1$, a main ingredient of ginseng root. *Neurosci. Res.* **1997**, *28*, 191–200.

(21) Yokozawa, T.; Satoh, A.; Cho, E. J. Ginsenoside-Rd attenuates oxidative damage related to aging in senescence-accelerated mice. *J. Pharm. Phamacol.* **2004**, *56*, 107–113.
(22) Kim, J. S.; Kim, K. W.; Choi, K. J.; Kwak, Y. K.; Im, K. S.; Lee, K. H.; Chung, H. Y. Screening of antioxidative components from red ginseng saponin. *Korean J. Ginseng Sci.* **1996**, *20*, 173–178.
(23) Kang, K. S.; Kim, H. Y.; Pyo, J. S.; Yokozawa, T. Increase in the free radical scavenging activity of ginseng by heat-processing. *Biol. Pharm. Bull.* **2006**, *29*, 750–754.
(24) Kang, K. S.; Yokozawa, T.; Kim, H. Y.; Park, J. H. Study on the nitric oxide scavenging effects of ginseng and its compounds. *J. Agric. Food Chem.* **2006**, *54*, 2558–2562.
(25) Xie, J. T.; Shao, Z. H.; Vanden Hoek, T. L.; Chang, W. T.; Li, J.; Mehendale, S.; Wang, C. Z.; Hsu, C. W.; Becker, L. B.; Yin, J. J.; Yuan, C. S. Antioxidant effects of ginsenoside Re in cardiomyocytes. *Eur. J. Pharmacol.* **2006**, *532*, 201–207.
(26) Rosenkranz, A. R.; Schmaldienst, S.; Stuhlmeier, K. M.; Chen, W.; Knapp, W.; Zlabinger, G. J. A microplate assay for the detection of oxidative products using 2′,7′-dichlorofluorescin-diacetate. *J. Immunol. Methods* **1992**, *156*, 39–45.
(27) Fujioka, N.; Yamasaki, K.; Kasai, R.; Tanaka, O.; Shoyama, Y.; Nishioka, I. Dammarane and Oleanane saponins from callus tissue of *Panax japonicus*. *Phytochemistry* **1989**, *28*, 1855–1858.
(28) Duc, N. M.; Kasai, R.; Ohtani, K.; Ito, A.; Nham, N. T.; Yamasaki, K.; Tanaka, O. Saponins from Vietnamese ginseng, *Panax vietnamensis* Ha et Grushv. Collected in central Vietnam. II. *Chem. Pharm. Bull.* **1994**, *42*, 115–122.
(29) Qiu, F.; Ma, Z. Z.; Xu, S. X.; Yao, X. S.; Che, C. T.; Chen, Y. J. A pair of 24-hydroperoxyl epimeric dammarane saponins from flower-buds of *Panax ginseng*. *J. Asian Nat. Prod. Res.* **2001**, *3*, 235–240.
(30) Morikawa, T.; Xu, F.; Kashima, Y.; Matsuda, H.; Ninomiya, K.; Yoshikawa, M. Novel dolabellane-type diterpene alkaloids with lipid metabolism promoting activities from the seeds of *Nigella sativa*. *Org. Lett.* **2004**, *6*, 869–872.
(31) Ko, S. R.; Suzuki, Y.; Suzuki, K.; Choi, K. J.; Cho, B. G. Marked Production of Ginsenosides Rd, $F_2$, $Rg_3$, and compound K by enzymatic method. *Chem. Pharm. Bull.* **2007**, *55*, 1522–1527.
(32) Mosmann, T. Rapid colorimetric assay for cellular growth and survival: Application to proliferation and cytotoxicity assays. *J. Immunol. Methods* **1983**, *65*, 55–63.

**Received for review September 22, 2009. Revised manuscript received November 17, 2009. Accepted December 7, 2009. This study was supported by the Technology Development Program for Agriculture and Forestry (No. 108079-3), the Ministry for Agriculture, Forestry and Fisheries; and the Priority Research Center Program through the National Research Foundation of Korea (NRF) funded by the Ministry of Education, Science and Technology (2009-0093815), Republic of Korea.**